AZD0364 Is a Potent and Selective ERK1/2 Inhibitor That Enhances Antitumor Activity in *KRAS*-Mutant Tumor Models when Combined with the MEK Inhibitor, Selumetinib

Vikki Flemington[1], Emma J. Davies[1], David Robinson[1], Linda C. Sandin[1], Oona Delpuech[1], Pei Zhang[1], Lyndsey Hanson[1], Paul Farrington[1], Sigourney Bell[1], Katarzyna Falenta[1], Francis D. Gibbons[2], Nicola Lindsay[2], Aaron Smith[2], Joanne Wilson[2], Karen Roberts[3], Michael Tonge[3], Philip Hopcroft[3], Sophie E. Willis[4], Martine P. Roudier[4], Claire Rooney[4], Elizabeth A. Coker[5], Patricia Jaaks[5], Mathew J. Garnett[5], Stephen E. Fawell[6], Clifford D. Jones[7], Richard A. Ward[8], Iain Simpson[7], Sabina C. Cosulich[6], J. Elizabeth Pease[6], and Paul D. Smith[1]

ABSTRACT

The RAS-regulated RAF–MEK1/2–ERK1/2 (RAS/MAPK) signaling pathway is a major driver in oncogenesis and is frequently dysregulated in human cancers, primarily by mutations in *BRAF* or *RAS* genes. The clinical benefit of inhibitors of this pathway as single agents has only been realized in *BRAF*-mutant melanoma, with limited effect of single-agent pathway inhibitors in *KRAS*-mutant tumors. Combined inhibition of multiple nodes within this pathway, such as MEK1/2 and ERK1/2, may be necessary to effectively suppress pathway signaling in *KRAS*-mutant tumors and achieve meaningful clinical benefit. Here, we report the discovery and characterization of AZD0364, a novel, reversible, ATP-competitive ERK1/2 inhibitor with high potency and kinase selectivity. *In vitro*, AZD0364 treatment resulted in inhibition of proximal and distal biomarkers and reduced proliferation in sensitive *BRAF*-mutant and *KRAS*-mutant cell lines. In multiple *in vivo* xenograft models, AZD0364 showed dose- and time-dependent modulation of ERK1/2-dependent signaling biomarkers resulting in tumor regression in sensitive *BRAF*- and *KRAS*-mutant xenografts. We demonstrate that AZD0364 in combination with the MEK1/2 inhibitor, selumetinib (AZD6244 and ARRY142886), enhances efficacy in *KRAS*-mutant preclinical models that are moderately sensitive or resistant to MEK1/2 inhibition. This combination results in deeper and more durable suppression of the RAS/MAPK signaling pathway that is not achievable with single-agent treatment. The AZD0364 and selumetinib combination also results in significant tumor regressions in multiple *KRAS*-mutant xenograft models. The combination of ERK1/2 and MEK1/2 inhibition thereby represents a viable clinical approach to target *KRAS*-mutant tumors.

Introduction

The RAS-regulated RAF–MEK1/2–ERK1/2 (RAS/MAPK) signaling pathway is a fundamental signaling pathway in many cell types, regulating cell-cycle progression, apoptosis, differentiation, and cell motility (1, 2). In normal physiologic conditions, the RAS/MAPK pathway is activated by receptor tyrosine kinases, such as EGFR and FGFR. When bound to their ligands, these receptors recruit guanine nucleotide exchange factors, such as SOS, to the membrane, which in turn activate RAS proteins by exchange of GDP for GTP. RAS-GTP causes the dimerization of RAF protein kinases that phosphorylate MEK1 and MEK2 (*MAP2K1* and *MAP2K2*), which then phosphorylates ERK1 and ERK2 (*MAPK3* and *MAPK1*), the downstream effector protein kinases of the pathway. ERK1 and ERK2 have hundreds of direct substrates, including p90RSK and FRA1, that are responsible for eliciting the effects of the pathway (3). RAS/MAPK signaling is frequently dysregulated in cancer, with mutations in the *RAS* genes present in 27% of all cancers (4, 5). The high prevalence of RAS/MAPK pathway dysregulation in cancer coupled with the chemically tractable protein targets in this pathway has led to the discovery of numerous small-molecule inhibitors that target the three key nodes in this pathway, RAF (6), MEK (7), and ERK (8).

Despite many clinical trials in an array of cancer indications, inhibitors of the RAS/MAPK pathway as single agents have only been approved for the treatment of *BRAF*-mutant melanoma (6, 9). The reasons for limited clinical benefit of single-agent pathway inhibitors are complex, however, it is evident that reactivation of the RAS/MAPK pathway plays a key role. For example, in *BRAF*-mutant melanoma, pathway reactivation is known to occur through genetic alterations in the pathway that override BRAF inhibition, for example, *NRAS*

[1]Bioscience, Oncology R&D, AstraZeneca, Cambridge, England, United Kingdom. [2]DMPK, Oncology, Oncology R&D, AstraZeneca, Cambridge, England, United Kingdom and Waltham, Massachusetts. [3]Discovery Science, BioPharmaceuticals R&D, AstraZeneca, Cambridge, England, United Kingdom. [4]Translational Medicine, Oncology R&D, AstraZeneca, Cambridge, England, United Kingdom. [5]Wellcome Sanger Institute, Cambridge, England, United Kingdom. [6]Oncology R&D, AstraZeneca, Waltham, England, United Kingdom. [7]Former employee of AstraZeneca. [8]Medicinal Chemistry, Oncology R&D, AstraZeneca, Cambridge, England, United Kingdom.

Note: Supplementary data for this article are available at Molecular Cancer Therapeutics Online (http://mct.aacrjournals.org/).

V. Flemington and E.J. Davies contributed equally to this article.

Current address for C.D. Jones: RedX Pharma, Cheshire, United Kingdom; current address for I. Simpson: Vertex Pharmaceuticals, Oxford, United Kingdom.

Corresponding Author: Vikki Flemington, AstraZeneca, Cambridge, England CB2 0RE, United Kingdom. Phone: 44-1625-234570; E-mail: vikki.flemington@astrazeneca.com

Mol Cancer Ther 2021;20:238–49

doi: 10.1158/1535-7163.MCT-20-0002

mutation, *BRAF* amplification, and *BRAF* splice variants (10–12). This has led to the approval of combined MEK and BRAF inhibition in $BRAF^{V600E/K}$-mutant melanoma and $BRAF^{V600E}$-mutant non–small cell lung cancer (NSCLC; refs. 13–17). In RAS-driven disease, profound relief of feedback inhibition is considered to be a major limitation to single-agent inhibitor efficacy (7, 18, 19). Combined inhibition of multiple nodes within the RAS/MAPK pathway may be necessary to effectively suppress pathway signaling and achieve meaningful clinical benefit, specifically in patients with *KRAS*-mutant tumors where single agents have not been effective. Targeting the effector kinase of the pathway, ERK1/2, could provide a way of both controlling the output of the dysregulated pathway and preventing reactivation of the pathway (8, 20, 21).

To this end, we have developed AZD0364, a novel, potent, ATP competitive, and highly selective inhibitor of ERK1 and ERK2. Here, we report the preclinical characterization of AZD0364 in preclinical models with aberrant RAS/MAPK pathway mutations, including *BRAF*- and *KRAS*-mutant cell lines and xenograft models. In all preclinical models tested, AZD0364 robustly inhibited phosphorylation of target substrates and RAS/MAPK pathway–dependent transcriptional output. The treatment-dependent effect upon ERK1/2 phosphorylation by AZD0364 varied across different cell lines. In a subset of *KRAS*-mutant NSCLC cell lines, combined treatment with AZD0364 and selumetinib was highly synergistic and resulted in deeper and more durable suppression of the RAS/MAPK pathway that was superior to single-agent treatment. This drug combination also significantly suppressed RAS/MAPK pathway output and tumor growth *in vivo* to a greater extent than achievable with the MTDs of either agent given as a monotherapy. These data demonstrate that combined AZD0364 and selumetinib effectively suppresses RAS/MAPK pathway signaling and delivers durable regressions in *KRAS*-mutant preclinical models.

Materials and Methods

Additional methods can be found in the Supplementary Materials and Methods section. Detailed methods for X-ray crystallography, the CDK2:cyclin E electromobility shift assay, and ERK and MEK biochemical and cellular assays are described in our previous publications (22, 23).

Kinase selectivity assays

Broad kinase selectivity was determined in a 122-assay panel of human wild-type (WT) kinase assays (binding and/or activity) available from the Thermo Fisher Scientific SelectScreen Kinase Profiling service (https://www.thermofisher.com/uk/en/home/products-and-services/services/custom-services/screening-and-profiling-services/selectscreen-profiling-service/selectscreen-kinase-profiling-service.html).

Western blot analysis

Detailed methodology can be found in the Supplementary Materials and Methods. Cells were seeded into 6-well plates and left to attach overnight. The following day, the cells were treated with AZD0364 and/or selumetinib for the indicated concentrations and time. Western blotting was carried out from lysates of these cells and probed using the following antibodies: p-ERK1/2 (T202/Y204, #9101), ERK1/2 (#4696), p-MEK1/2 (S221,#2338), MEK1/2 (#4694) p-p90RSK (T359, #8753), FRA1 (#5281), p-FRA1 (S265, #3880), cleaved PARP (#5625), BIM (#2933), and p27 (#3686) all obtained from Cell Signaling Technology. The p90RSK antibody was obtained from BD Bioscience (#610226) and the vinculin antibody was obtained from Sigma (#V9131).

For Western blot analysis from *in vivo* experiments, frozen tumor samples were homogenized in lysis buffer (as detailed in Supplementary Materials and Methods) in 2 mL lysing matrix A tubes (Precellys). Protein quantification and Western blotting were carried out following the same protocol detailed in the Supplementary Materials and Methods. The following antibodies were used: p-p90RSK (S363, T359, clone E238, #32413, Abcam) and p-FRA1 (S265, #3880, Cell Signaling Technology) and loading control vinculin (clone SPM227, #18058, Abcam). Immunoblots were visualized and band intensity was quantified using the Syngene GeneTools Software (Syngene). Data were visualized using GraphPad prism version 8.0.0 for Windows (GraphPad Software) and statistical differences between vehicle and treatment groups were determined using one-way ANOVA.

In vivo efficacy and target engagement studies

Athymic Nude-$Foxn1^{nu}$ mice (Envigo) were group housed under specific pathogen-free conditions in individually Ventilated Cages (Techniplast) at Alderley Park (England, United Kingdom). Mice had access to water and food *ad libitum*. Experiments were conducted in 8- to 12-week-old female mice in full accordance with the United Kingdom Home Office Animal (Scientific Procedures) Act 1986. Mice were inoculated subcutaneously with 100 μL of the following cell lines: Calu-6 [1×10^6 cells/mouse mixed with a 1:1 ratio in Matrigel (BD Biosciences)], A549 (5×10^6 cells/mouse, 1:1 ratio with Matrigel), A375 (1×10^7 cells/mouse in 50 μL volume), A375 PLX/Sel-R1 (5×10^6 cells/mouse), HCT-116 (3×10^6 cells/mouse, 1:1 ratio with Matrigel), and NCI-H358 (3×10^6 cells/mouse, 1:1 ratio with Matrigel). Tumor growth was monitored twice weekly via caliper measurement and tumor volume was calculated using the formula: $3.14 \times \text{length} \times \text{width}^2/6{,}000$. Growing tumors were randomized and recruited onto study when they reached an average of approximately 0.4 cm^3 for target engagement studies and approximately 0.2 cm^3 for efficacy studies. AZD0364 was formulated in 10% DMSO and 90% of 40% KLEPTOSE, and selumetinib was formulated in 0.5% METHOCEL (hydroxypropyl methocellulose)/0.1% polysorbate 80. All drugs were administered via the oral route. Bodyweights and tumor measures were taken at least twice weekly. For efficacy experiments, tumor growth of each treatment group was represented graphically as geomeans ± SEM, using GraphPad Prism version 8.0.0 for Windows (GraphPad Software). Tumor growth inhibition (TGI) and tumor regressions were calculated by comparing relative tumor volumes, the Student *t* test (one-sided) was used to determine significance.

In vivo drug quantification

Whole-blood samples for plasma pharmacokinetics analysis were taken via venapuncture of the tail vein (20 μL of whole blood), whole blood was mixed 1:5 with PBS, centrifuged at $1{,}500 \times g$ for 3 minutes at 4°C, and the supernatant was extracted. Each sample (25 μL) was prepared using an appropriate dilution factor and compared against an 11-point standard calibration curve (1–10,000 nmol/L) prepared in DMSO and spiked into blank plasma. Acetonitrile (100 μL) was added with the internal standard, followed by centrifugation at 3,000 rpm for 10 minutes. Supernatant (50 μL) was then diluted in 300 μL water and analyzed via ultra performance liquid chromatography–tandem mass spectrometry (UPLC/MS-MS).

Results

Discovery and initial characterization of the novel ERK1/2 inhibitor, AZD0364

We have reported previously the discovery of compound 35 (24) as a potent and selective inhibitor of ERK1/2, which was optimized from a

chemical start point with suboptimal selectivity. Following extensive optimization of a lead series developed from compound 35 (23), a novel, selective, and potent ERK1/2 inhibitor, AZD0364, was identified (**Fig. 1A**). The binding mode of AZD0364 in ERK2 as determined by X-ray crystallography demonstrates binding of AZD0364 in the ATP binding site (**Fig. 1B**). AZD0364 had an activity of 0.66 nmol/L in an ERK2 biochemical assay [run at 1 mmol/L (Km) ATP], compared with 0.39 nmol/L for SCH772984, 16.7 nmol/L for GDC-0994, and 1.7 nmol/L for BVD-523 (23). In addition, an imaging-based high-throughput assay measuring levels of phosphorylated p90RSK (phospho-p90RSK) and phosphorylation of ERK1/2 (phospho-ERK) was performed in an A375 melanoma cell line containing a $BRAF^{V600E}$ mutation. AZD0364 inhibits p90RSK phosphorylation with an IC_{50} value of 5.73 nmol/L, therefore, demonstrating that AZD0364 potently inhibits the catalytic function of ERK1/2. This value is comparable with or less than for the reported ERK1/2 competitors, SCH772984, GDC-0994, and BVD-523 (ulixertinib), for which we have calculated IC_{50} values for p90RSK phosphorylation as 12.2, 86.1, and 155 nmol/L, respectively (**Fig. 1C**). In the same assay system, AZD0364 inhibits ERK1/2 phosphorylation, with an IC_{50} of 1.73 nmol/L, which also suggests that AZD0364 can prevent the activation of ERK1/2. The calculated IC_{50} of ERK1/2 phosphorylation by SCH772984 is 2.52 nmol/L, whereas we have calculated this value as 3.13 μmol/L for BVD-523, which agrees with the reported profiles of ERK1/2 inhibition by both agents (25, 26). Furthermore, treatment of A375 cells with BVD-523 results in elevated levels of phosphorylated ERK1/2 in the nucleus compared with DMSO-treated cells, whereas treatment with AZD0364 decreases levels of phosphorylated ERK1/2 (Supplementary Fig. S1A and S1B).

AZD0364 binds similarly to ERK1 and ERK2, with *K*d values of 3.9 and 3.8 nmol/L, respectively. To investigate wider kinase selectivity, AZD0364 was screened in a panel of 122 WT human kinases. AZD0364 was highly selective for ERK1/2 (**Fig. 1D**), with activity (stated as ≥80% inhibition/binding at 1 μmol/L) against only five other kinase assays in this panel: MEK1, BRAF, c-RAF, CDK2, and ARK5 (Supplementary Fig. S1C). AZD0364 was also screened in a broader panel of 353 human kinases, with activity against only nine other kinases in this panel: MEK1, COT, BRAF, MEK2, c-RAF, ERK7, CDK2, CDK5, and ARK5 (23). The MEK1, BRAF, and c-RAF assays listed are coupled pathway assays, using ERK2 protein as part of the assay cascade, therefore, an inhibitor of ERK2 will show activity in these assays. In subsequent testing, the IC_{50} of AZD0364 in an ARK5 assay was 0.4 μmol/L (Supplementary Fig. S1D). In-house biochemical testing was subsequently carried out to ensure that these compounds were not active against MEK1 or CDK2; AZD0364 was inactive against MEK1 at the dose range tested (>10 μmol/L) and showed minimal activity of 1 μmol/L against CDK2-cyclin E (Supplementary Fig. S1D).

AZD0364 directly modulates RAS/MAPK pathway signaling

To further characterize the mechanism of action and effects on signaling elicited by AZD0364, cell lines were selected on the basis of varying sensitivities to ERK1/2 inhibition as determined by the GI_{50} values, as shown in **Fig. 1C**; A375 ($BRAF^{V600E}$)-mutant melanoma cells (0.0592 μmol/L) and Calu-6 ($KRAS^{Q61K}$)-mutant NSCLC cells (0.173 μmol/L). The GI_{50} value for the A549 ($KRAS^{G12S}$)-mutant NSCLC cells was determined to be 0.32 μmol/L via multiple testing by using the same assay conditions. For this panel of cell lines, we classified the A375 $BRAF^{V600E}$-mutant cell line as sensitive to AZD0364, and the Calu-6 $KRAS^{Q61K}$ cell line as being more sensitive than the A549 $KRAS^{G12S}$ cell line (potency order of AZD0364: A375 0.0592, Calu-6 0.173, and A549 0.32 μmol/L).

In AZD0364-treated A375, Calu-6, and A549 cells, phosphorylation of the direct ERK1/2 substrate, p90RSK, was reduced in a dose-dependent manner at both 2 and 24 hours, which is consistent with sustained inhibition, as determined by Western blot analysis (**Fig. 2**). Phosphorylation of another direct ERK1/2 substrate, FRA1, was reduced to a greater extent at 24 hours posttreatment with AZD0364, compared with 2 hours posttreatment. This is coincident with a reduction in total FRA1 levels at 24 hours. Levels of FRA1 expression and stability have been shown to be regulated by ERK1/2 (27). In AZD0364-treated A549 cells, a reduction of p90RSK and FRA1 phosphorylation was evident at both timepoints. However, this was to a lesser extent than in A375 and Calu-6 cells.

In both the A375 and Calu-6 cell lines, 24 hours treatment with AZD0364 resulted in a dose-dependent increase in the proapoptotic protein BIM splice variant, BIM-EL, and the marker of apoptosis, cleaved PARP. In addition, the cell-cycle inhibitor protein, p27, showed a similar pattern of increase, thus indicating a direct impact of ERK1/2 inhibition on the cell cycle in these cell lines. In contrast, in the less sensitive A549 cell line, no increase was seen in cleaved PARP or BIM-EL, and only a marginal increase of p27, despite the modulation of ERK target proteins, p90RSK and FRA1 (**Fig. 2C**). Pathway reactivation, indicated by increased levels of phosphorylated MEK at doses where inhibition of p90RSK and FRA1 phosphorylation was seen, was apparent after 2 and 24 hours treatment with AZD0364 in both the *KRAS*-mutant cells lines (Calu-6 and A549), but not in *BRAF*-mutant cells (A375), consistent with previous studies (**Fig. 2C**; Supplementary Fig. S2A; refs. 7, 18, 28). In A375 and Calu-6 cell lines there was no significant impact of AZD0364 on phosphorylated ERK1/2, however, in A549 cells, a dose-dependent increase in phosphorylated ERK1/2 was evident at both 2 and 24 hours posttreatment with AZD0364 (**Fig. 2C**; Supplementary Fig. S2A). Together, these data demonstrate that the impact of AZD0364 on phosphorylation of ERK1/2 is different across cell lines. The A375 ($BRAF^{V600E}$)-mutant melanoma cell line was used in a cellular screening assay, in which modulation of phosphorylated p90RSK and ERK1/2 was detected in the same image. In the imaging assay, AZD0364 robustly inhibited both phosphorylation of p90RSK and ERK1/2, which indicates that AZD0364 inhibits the catalytic function and prevents the activation of ERK1/2 (**Fig. 1C**; Supplementary Fig. S1A and S1B). However, by Western blotting, modulation of ERK1/2 phosphorylation by AZD0364 was not evident in A375 cells or Calu-6 cells (**Fig. 2A** and **B**). Qualitatively, we show that AZD0364 has a different effect on ERK1/2 phosphorylation to the reported ERK inhibitor, SCH772984, as detected by Western blotting in $KRAS^{G12C}$-mutant NSCLC H358 cells (Supplementary Fig. S1E). However, the downstream modulation of phosphorylation of the direct ERK substrates, p90RSK and FRA1, was consistent across cell lines and technologies. Therefore, AZD0364-induced inhibition of p90RSK and FRA1 phosphorylation, as proximal biomarkers of ERK1/2 inhibition, was measured in subsequent studies.

To further investigate cellular phenotypic responses to ERK1/2 inhibition, AZD0364 was profiled in 72-hour cell proliferation screen of 747 fully characterized cancer cell lines (29). Cell lines with a GI_{50} value of <1 μmol/L were classified as sensitive to AZD0364. Of the 747 cell lines tested, 56 cell lines were sensitive to AZD0364 (Supplementary Table S2), the sensitivity profile of these lines is shown in **Fig. 3A**. To identify genomic features associated with sensitivity to AZD0364, an ANOVA test was used to correlate drug response (GI_{50} values) with genomic alterations across the panel. These genomic alterations included: point mutations, recurrent copy number–altered chromosomal segments, and selected cancer gene rearrangements. Cell lines with mutations in *BRAF* or *NRAS* were strongly associated with

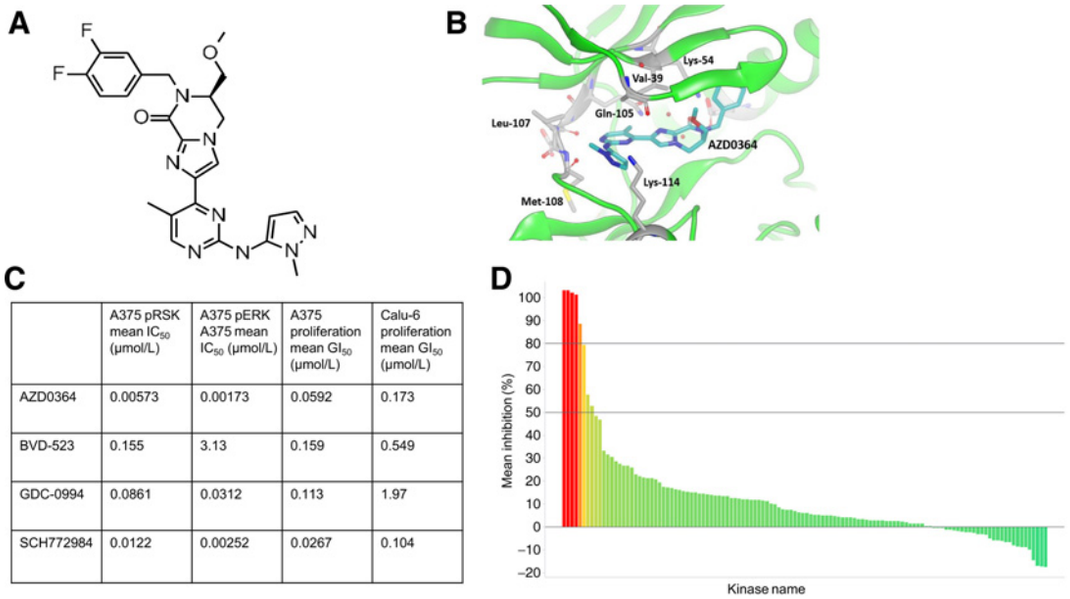

	A375 pRSK mean IC_{50} (μmol/L)	A375 pERK A375 mean IC_{50} (μmol/L)	A375 proliferation mean GI_{50} (μmol/L)	Calu-6 proliferation mean GI_{50} (μmol/L)
AZD0364	0.00573	0.00173	0.0592	0.173
BVD-523	0.155	3.13	0.159	0.549
GDC-0994	0.0861	0.0312	0.113	1.97
SCH772984	0.0122	0.00252	0.0267	0.104

Figure 1.
AZD0364: structure, binding mode, potency, and selectivity profile. **A,** Chemical structure of AZD0364. **B,** Crystal structure of AZD0364 bound to the ATP binding site of ERK2. **C,** Summary table of biochemical and cellular potency of AZD0364 and reported ERK1/2 inhibitors. **D,** Kinases in the Thermo Fisher Scientific 122-kinase panel that showed greater than 80% inhibition/binding after 1 μmol/L treatment with AZD0364 are highlighted in red and listed in Supplementary Fig. S1C.

sensitivity to AZD0364, presented as a volcano plot of *P* value versus effect size (**Fig. 3B**). *KRAS*-mutant cell lines were also associated with sensitivity to AZD0364, but the log *P* value and effect size were not as great as *BRAF* and *NRAS*. Furthermore, GI_{50} values were plotted of *BRAF*-, *NRAS*-, and *KRAS*-mutant cell lines versus WT (**Fig. 3C**), where WT was all cell lines screened that did not contain mutations in these three genes. The average GI_{50} values for *BRAF*-, *NRAS*-, and *KRAS*-mutant cell lines were lower than the WT cell lines, however, there was significant variability in the potency of growth inhibition within each subset of cell lines with mutations in *BRAF, NRAS*, and *KRAS*. This screen was also carried out with reported clinical stage ERK inhibitors: BVD-523, SCH772984, and GDC-0994, the calculated AUC values for AZD0364 showed good correlation with BVD-523 (Supplementary Fig. S2A).

AZD0364 demonstrates *in vivo* antitumor activity in *KRAS*- and *BRAF*-mutant cancer cell line xenograft models

On the basis of our *in vitro* findings that AZD0364 reduced proliferation and inhibited multiple pathway biomarkers in a concentration-dependent manner, we evaluated the activity of AZD0364 in A375 ($BRAF^{V600E}$), Calu-6 ($KRAS^{Q61K}$), and A549 ($KRAS^{G12S}$) cancer cell lines grown as xenografts in nude mice. The relationship between pharmacokinetics and pharmacodynamics was established in the Calu-6 cell line. AZD0364 has a half-life of approximately 2.5 hours

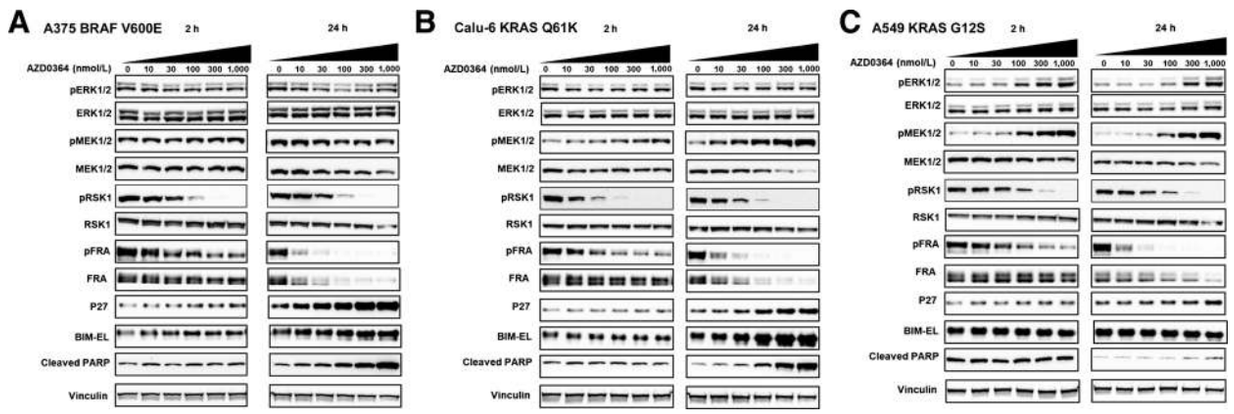

Figure 2.
AZD0364 reduces RAS/MAPK pathway output in a time- and dose-dependent manner in both *BRAF*- and *KRAS*-mutant cancer cell lines. Immunoblots of whole-cell lysates prepared from A375 (**A**), Calu-6 (**B**), and A549 (**C**) cell lines. Cells were treated with AZD0364 at the indicated concentrations for 2 and 24 hours. Western blots are representative of at least two experiments.

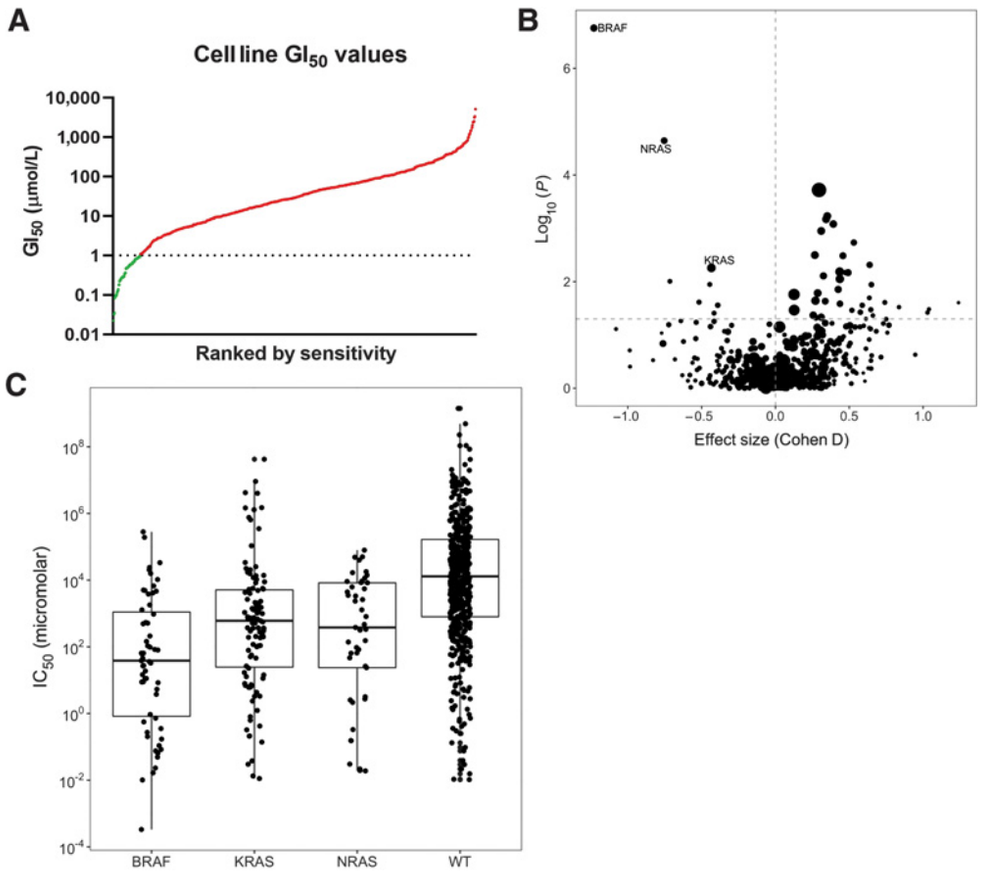

Figure 3.

BRAF and *NRAS* mutations confer sensitivity to AZD0364. **A,** Ranked GI_{50} values for AZD0364 across 747 cancer cell lines; dotted line indicates GI_{50} sensitivity cutoff of <1 μmol/L. Sensitive cell lines are highlighted in green. **B,** Volcano plot of *P* value versus effect size for each cell line; dashed lines indicate cutoffs for log10 (*P*) and effect size that are considered significant. Sensitive cell lines have a negative Cohen D value. **C,** AZD0364 growth inhibition GI_{50} values in *BRAF*-, *NRAS*-, and *KRAS*-mutant cell lines versus WT (non-*BRAF*-, *NRAS*-, *KRAS*-mutant) cell lines.

in mouse when dosed at 50 mg/kg orally, plasma concentrations of AZD0364 were compared with levels of phosphorylated p90RSK (phospho-p90RSK) and phosphorylated FRA1 (pFRA1) in the tumor over a 24-hour period following a single 50 mg/kg oral dose of AZD0364 (**Fig. 4A**). In addition, biomarkers of transcriptional changes in the tumor, DUSP6 and ETV4, were quantified by qRT-PCR (**Fig. 4B**). Modulation of *DUSP6* and *ETV4* gene expression is predictive of RAS/MAPK pathway inhibition (30, 31) and, therefore, serves as an additional measure of pathway output. Modulation of all biomarkers tested was found to be directly related to exposure and recovered to baseline levels in a time-dependent manner (**Fig. 4A** and **B**; Supplementary Fig. S3A–S3C).

AZD0364 induced significant TGI of 100% upon continuous daily dosing of 50 mg/kg for 21 days in the A375 ($BRAF^{V600E}$) and Calu-6 ($KRAS^{Q61K}$) xenograft models when compared with the control group ($P < 0.001$), both tumor models showed regression from baseline (**Fig. 4C** and **D**). AZD0364 was efficacious in the A549 ($KRAS^{G12S}$) xenograft model, with a significant TGI of 68% at day 20 when compared with the control group (p value < 0.001; **Fig. 4E**). However, tumor regressions were not observed in this model, which is consistent with the lower sensitivity and lack of effect on apoptotic markers *in vitro* of this cell line compared with A375 and Calu-6. No significant body weight changes were observed in these models (less than 10% of starting body weight; Supplementary Fig. S3D–S3G). These data further demonstrate the variability of response to AZD0364 in *KRAS*-mutant cell lines.

To understand the dose and schedule requirements for efficacy of AZD0364, several different dosing regimens were explored in the Calu-6 xenograft model (**Fig. 4F**). A clear dose response was observed when dosing both once daily and twice daily. Dosing 12.5 mg/kg twice daily resulted in equivalent antitumor activity to 50 mg/kg once daily, with regressions from baseline of 51% and 49%, respectively. In addition, dosing 50 mg/kg once daily 3 days on and 4 days off, or 25 mg/kg twice daily 3 days on and 4 days off was equivalent [TGI of 100% (5% regression) and 99%, respectively]. For all doses, no significant body weight changes were observed (Supplementary Fig. S3H). In this model, the efficacy of both twice daily and once daily dosing was equivalent, intermittent dosing resulted in more modest efficacy compared with continuous treatment.

In addition, AZD0364 was tested in an A375 cell line model which has developed acquired resistance to both the BRAF inhibitor, PLX-4720, and the MEK inhibitor, selumetinib (A375 PLX/Sel-R1). This cell line carries $BRAF^{V600E}$, $NRAS^{Q61R}$, and $MEK1^{Q56P}$ mutations (32). AZD0364 suppressed phosphorylation of p90RSK and FRA1 and

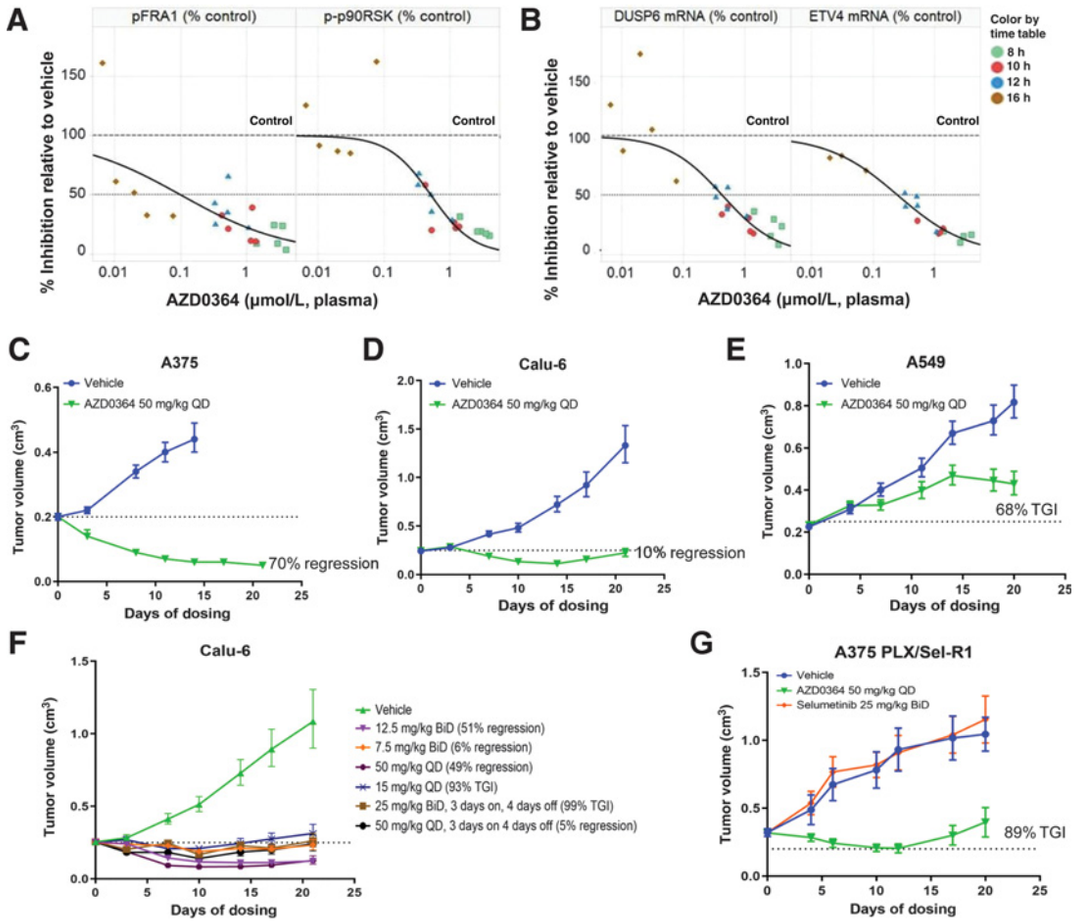

Figure 4.

In vivo antitumor efficacy of AZD0364 in RAS/MAPK-driven tumor models. **A,** Pharmacokinetic/pharmacodynamic relationship between AZD0364 blood-free plasma concentrations and downstream protein targets of ERK1/2, pFRA1, and p-p90RSK. **B,** Pharmacokinetic/pharmacodynamic relationship between AZD0364 blood-free plasma concentrations and downstream transcriptional targets of ERK1/2, DUSP6, and ETV4. Antitumor efficacy of AZD0364 at 50 mg/kg once daily (QD) treatment in A375 melanoma xenograft (mouse/group, $n = 10$), 70% regression from baseline on day 21 (**C**), Calu-6 NSCLC xenograft (mouse/group, $n = 11$), 10% regression reached from baseline on day 21 (**D**), and A549 NSCLC xenograft (mouse/group, $n = 12$), 68% TGI from baseline on day 21 (**E**). **F,** Efficacy of AZD0364 at various dosing schedules in the Calu-6 NSCLC xenograft (mouse/group, $n = 10$). **G,** Efficacy of AZD0364 in A375 xenograft model with acquired resistance to BRAF and MEK inhibition (mouse/group, $n = 10$), 89% TGI from baseline on day 21. All data are presented as mean ± SEM. BiD, twice daily.

caused an accumulation of apoptotic and cell-cycle inhibition markers in this cell line *in vitro* (Supplementary Fig. S4). *In vivo* tumor growth was suppressed significantly at the end of the treatment period in animals treated with AZD0364 compared with those treated with selumetinib, with a significant TGI of 89% at day 20 when compared with the control group (p value < 0.01; **Fig. 4G**). Therefore, we have demonstrated that MEK/RAF inhibitor resistance is driven by RAS/MAPK pathway reactivation in this model and can be overcome by inhibition of ERK1/2 with AZD0364.

Combination of AZD0364 and selumetinib has synergistic activity in *KRAS*-mutant cells and results in stronger suppression of RAS/MAPK pathway output

Calu-6 and A549 *KRAS*-mutant NSCLC cell lines, both *in vitro* and *in vivo*, showed differential responses to single-agent AZD0364 treatment. To determine whether there is a correlation between type of *KRAS* mutation and sensitivity to ERK inhibition, an extensive panel of 24 *KRAS*-mutant NSCLC cell lines was assembled to represent the different mutations in *KRAS* commonly detected in patients with NSCLC (ref. 33; Supplementary Table S3). In a 3-day cell growth assay, GI_{50} values for AZD0364 and the MEK1/2 inhibitor, selumetinib, were calculated (**Fig. 5A** and **B**), with cells with a $GI_{50} < 1$ μmol/L classified as sensitive. Consistent with the data from the 72-hour cell panel screen (**Fig. 3**), the response of *KRAS*-mutant cell lines to single-agent ERK1/2 or MEK1/2 inhibition was variable, with cell lines falling into both the sensitive and resistant categories. There was a significant correlation between single-agent response of the *KRAS*-mutant NSCLC cell lines to AZD0364 and selumetinib (Supplementary Fig. S5A).

To enhance the phenotypic response in this panel of *KRAS*-mutant NSCLC cell lines, AZD0364 and selumetinib were combined using a dose response of both agents in each cell line. A 6 × 6 dosing matrix was used and the resulting phenotypic data were modeled using the Loewe independence model, which provided a measure of synergistic combination response between the compounds which was calculated to be greater than an additive combination effect. Synergistic

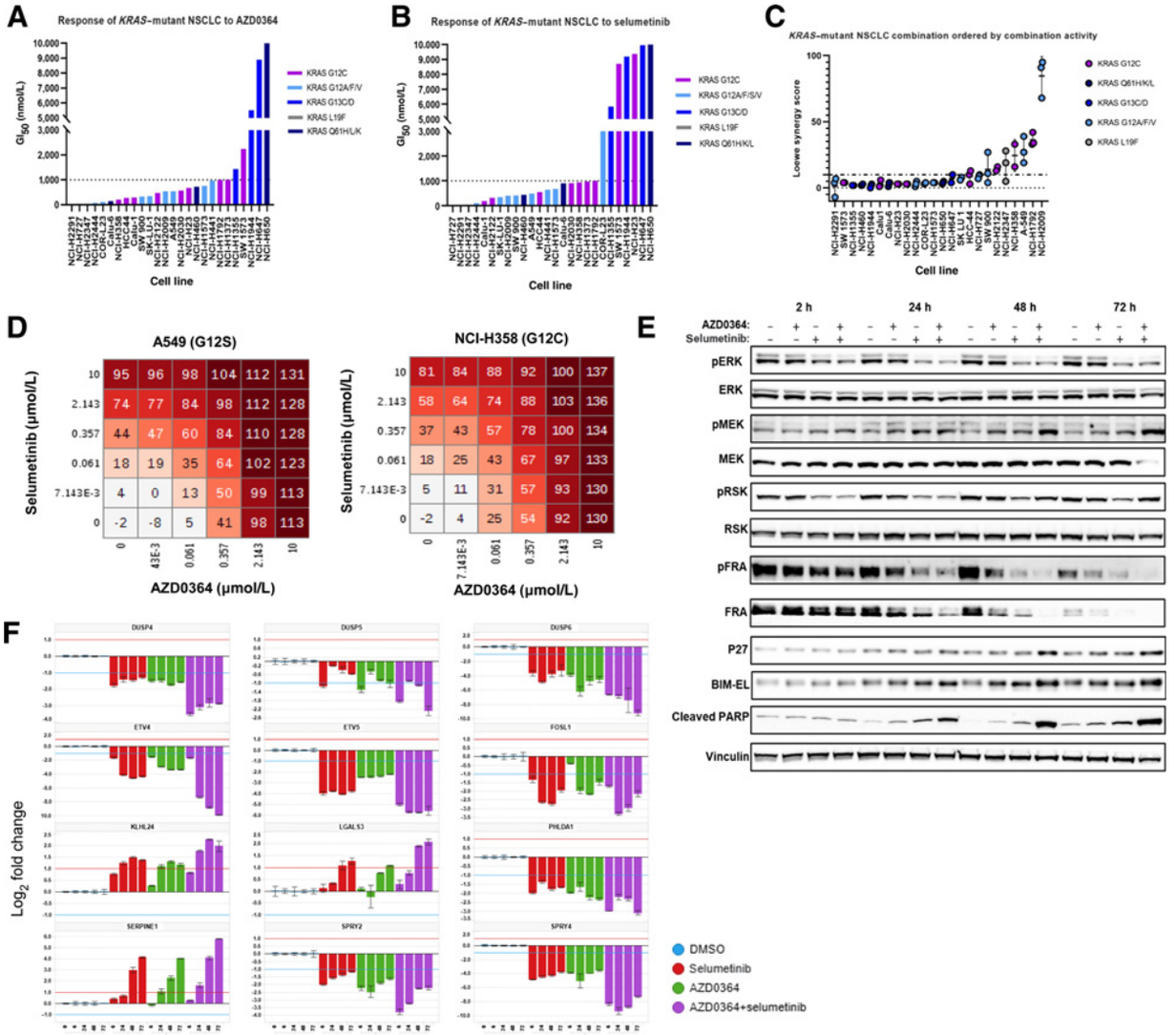

Figure 5.

Combined inhibition of ERK and MEK resulted in greater cell growth inhibition and greater downstream target modulation in *KRAS*-mutant NSCLC cell lines. Chart of growth inhibition (GI_{50}) values in a panel of *KRAS*-mutant NSCLC cell lines for AZD0364 (**A**) and selumetinib (**B**). **C,** Loewe synergy scores for combined treatment of AZD0364 and selumetinib in a panel of *KRAS*-mutant NSCLC cell lines. Synergistic combinations are defined to have a Loewe score of ≥5; dashed line indicates synergy score of 10. **D,** Representative dose matrices for A549 and NCI-H358 cell lines showing the percent growth inhibition on a scale of 0%–200%, with 0%–100% representing inhibition of cell growth and 100%–200% representing cell death, relative to the day 0 values. **E,** Immunoblot from A549 NSCLC cells treated with 0.03 μmol/L AZD0364 and 0.03 μmol/L selumetinib as a single agents and in combination. **F,** Expression of selected RAS/MAPK-related transcripts was quantified by qRT-PCR in A549 NSCLC cells treated with AZD0364 and/or selumetinib, both at 500 nmol/L for 6, 24, 48, and 72 hours. Blue/red line indicates a 2-fold change in gene expression. These changes were significantly altered from the control for at least two timepoints, $P < 0.05$, pairwise Student *t* test.

combinations are defined to have a Loewe score of ≥5. As shown in **Fig. 5C**, a subset of *KRAS*-mutant NSCLC cell lines showed a synergistic combination response to MEK and ERK inhibition. Two cell lines that demonstrated synergistic combination (A549 and NCI-H358) are exemplified in **Fig. 5D**, where the results are shown on a scale of 0%–200% growth inhibition, where 0%–100% indicates in inhibition of cell proliferation and 100%–200% indicates cell death has occurred. In A549 and NCI-H358 cells, combination treatment resulted in a growth inhibition value between 100% and 200%, which is associated with cell death, whereas single-agent treatment selumetinib does not and AZD0364 treatment only resulted in a growth inhibition value of >100% at 10 μmol/L. Therefore, this further analysis indicates a high Loewe synergy score correlates with a clear benefit of combination treatment over the duration of the assay period.

To further investigate the response of *KRAS*-mutant NSCLC cell lines to dual intra-RAS/MAPK pathway inhibition, AZD0364 was also combined with an alternative MEK inhibitor, trametinib, or a pan-RAF inhibitor. A similar pattern of response was seen across the cell panel (Supplementary Fig. S5B and S5C), which is consistent with our hypothesis that dual inhibition of the RAS/MAPK pathway is essential for maximal response in a subset of *KRAS*-mutant NSCLC cell lines.

To determine potential pharmacodynamic biomarkers of combination sensitivity, biomarkers of RAS/MAPK pathway activity, cell cycle, and apoptosis were quantified in the $KRAS^{G12S}$-mutant A549 cell line where synergy to the AZD0364 and selumetinib combination was observed. Dual treatment of AZD0364 and selumetinib resulted in a greater reduction of phosphorylation of the ERK1/2 target, FRA1, but not p90RSK, when compared with treatment with either single agent, when both inhibitors were used at 0.03 μmol/L (**Fig. 5E**). The reduction in phosphorylation of the downstream targets of ERK1/2 was sustained, with reductions maintained at the end of the treatment period (72 hours; **Fig. 5E**; Supplementary Fig. S5D). However, when the cells were treated with 0.3 μmol/L of each agent, there was also a modest, but sustained depletion of phospho-p90RSK in cells treated with the combination compared with single agent alone (Supplementary Fig. S5D). The consequences of relief of negative feedback were observed in terms of increases over time in the levels of phospho-MEK and partial recovery in the levels of phosho-p90RSK. At this higher drug concentration, single-agent treatment resulted in similar levels of pFRA1 depletion to combination treatment (Supplementary Fig. S5D). Combination treatment also resulted in an extended induction of the apoptotic markers, BIM-EL and cleaved PARP, and the cell-cycle inhibitor protein, p27.

To evaluate the impact of combination treatment on a panel of proximal biomarkers of the RAS/MAPK pathway, expression levels of 45 RAS/MAPK pathway–regulated genes were quantified by qRT-PCR. Expression of 19 of these genes was significantly modulated after combined AZD0364 and selumetinib treatment compared with single-agent treatment (statistical analysis of significantly modulated gene expression in Supplementary Fig. S5E). The time course of modulation is exemplified for 12 of these genes in **Fig. 5F**, all of which showed enhanced modulation at a minimum of two timepoints in cells treated with the combination compared with single agents. Broadly, these changes were sustained for the duration of the treatment (72 hours), and maximal modulation was observed in the combination-treated groups.

Several analyses were undertaken to identify defining features of *KRAS*-mutant NSCLC that respond to AZD0364 and selumetinib combination treatment. We were unable to determine a clear association between the individual *KRAS* mutation, or the existence of any concurrent mutation, present in the cell line and the response to either single-agent AZD0364 or selumetinib treatment, or the combination of both agents (**Fig. 5A–C**; Supplementary Table S3). To further investigate potential relationships between individual cell lines and sensitivity to an intrapathway combination, levels of basal pathway activation across this *KRAS*-mutant NSCLC cell line panel were determined by Western blotting. There was no clear association between individual protein levels of markers of pathway activation (phospho-p90SK), regulators of negative feedback (DUSP5 and DUSP6), or the apoptotic marker, BIM (Supplementary Fig. S5F), across the panel of *KRAS*-mutant NSCLC cell lines and the response to the combination of AZD0364 and selumetinib, as determined by the Loewe synergy score.

Combination of AZD0364 and selumetinib significantly enhances antitumor activity in *KRAS*-mutant tumor models

We have previously shown that the AZD0364 and selumetinib combination has an efficacious benefit over monotherapy in the A549 xenograft model (23). To validate this combination further, we tested it in the NCI-H358 ($KRAS^{G12C}$) NSCLC and the HCT-116 ($KRAS^{G13D}$) colorectal cancer *in vivo* xenograft models. Combined treatment of AZD0364 and selumetinib resulted in a strong regression effect that was durable over a 21-day period in both models (**Fig. 6A**). Tumors regressed from baseline by 65% in NCI-H358 and 58% in HCT-116 (p values < 0.001). There was a degree of bodyweight loss in the combination groups in the NCI-H358 experiment, and in the HCT-116 experiment, bodyweight loss was observed in all groups (Supplementary Fig. S6A and S6B). However, this weight loss was <15% and not considered to be significant. Robust pharmacodynamic modulation of p90RSK phosphorylation was observed in the combination groups at the end of study after 21 days of treatment (**Fig. 6B**).

In 21-day TGI studies, the *in vivo* dosing schedule of AZD0364 once daily and selumetinib twice daily involved administration of agents over an 8-hour period in the following 3× daily dosing schedule: [selumetinib (time t) + ERKi (t + 4 hour) + selumetinib (t + 8 hour)]. Therefore, to explore the modulation of downstream biomarkers in response to combination treatment in more detail, AZD0364 and selumetinib were dosed simultaneously for 6 days in the A549 xenograft model. With this dosing regimen, inhibition of p90RSK phosphorylation was not significantly reduced in the combination groups compared with single agents (**Fig. 6C**). However, IHC analysis showed enhanced suppression of the proliferation marker, Ki67, in the combination group compared with single-agent treatment (**Fig. 6D**; Supplementary Fig. S6C), consistent with the enhanced antitumor activity of the combination shown in this model. To investigate this observed difference in modulation of phosphorylation of the direct biomarker, p90RSK, and the more distal proliferation marker, Ki67, following 6 days of simultaneous combination treatment, expression levels of 45 RAS/MAPK pathway–regulated genes were quantified by qRT-PCR. The time course of modulation of the key RAS/MAPK–regulated genes *DUSP6, SPRED1, ETV4*, and *ETV5* is shown in **Fig. 6E**, all of which show enhanced modulation at a minimum of two timepoints after treatment with the combination compared with single agents. The statistical analysis of all significantly modulated gene expression changes is shown in Supplementary Fig. S6D. This enhanced modulation of transcript biomarkers in combination treatment correlates with greater modulation of the proliferation marker, Ki67, as shown by IHC. Taken together, these data show that in the A549 xenograft model, the distal transcript biomarkers of RAS/MAPK activity offer a more robust method of predicting combination benefit compared with the proximal phospho-p90RSK protein biomarker.

To further confirm that dual targeting of ERK and MEK nodes results in enhanced efficacy over single-node targeting, we replicated the thrice daily dosing schedule used for the combination with MEK inhibition alone, replacing the AZD0364 dose with a selumetinib dose: [MEKi (time t) + MEKi (t + 4 hours) + MEK*i* (t + 8 hours)]. Despite continuous cover over the GI_{50} with the [MEKi + MEKi + MEKi] schedule (Supplementary Fig. S6E), tumor regressions were not observed in contrast to the [MEKi (time t) + ERKi (t + 4 hours) + MEKi (t + 8 hours)] regimen; demonstrating enhanced efficacy can be achieved with dual RAS/MAPK pathway target inhibition compared with increasing the number of doses of a single agent (**Fig. 6F**). In addition, tumor regrowth (0.24 cm^3 at day 24 vs. 0.3 cm^3 at day 35) was evident in the selumetinib treatment group at day 35.

We observed increased bodyweight loss in the combination group over time (Supplementary Fig. S6F), some animals were terminated early because of progressive bodyweight loss. To overcome this, we evaluated an intermittent dosing schedule of the combination, with a 3.5-day dosing holiday occurring every 4th day of the study. Bodyweight loss was much less marked in the group that received the intermittent dosing schedule, with most animals returning to baseline weight when off drug, and only two animals having sustained bodyweight loss of >5% (Supplementary Fig. S6G). The intermittent dosing

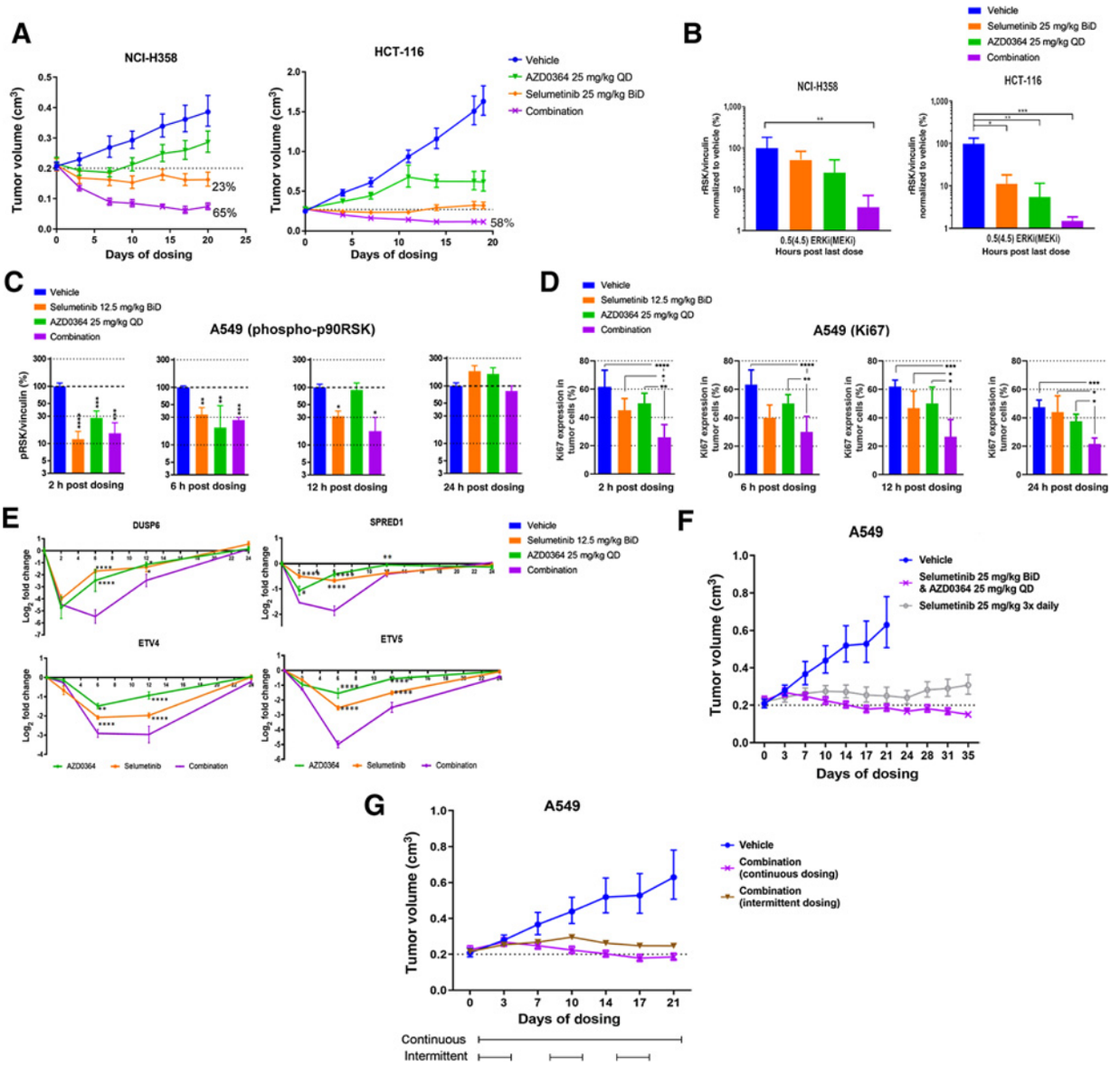

Figure 6.

Combined treatment of AZD0364 and selumetinib *in vivo*. **A,** Combined treatment of AZD0364 and selumetinib is more efficacious than single-agent treatment *in vivo* in NCI-H358 (mouse/group, $n = 6$–10) NSCLC and HCT-116 (mouse/group, $n = 12$) colorectal cancer tumor models. **B,** phospho-p90RSK expression was quantified by Western blotting from tumor samples taken after 21 days of dosing. **C,** phospho-p90RSK expression was quantified by Western blotting from A549 tumor samples taken after 6 days of dosing, AZD0364 and selumetinib dosed simultaneously. **D,** Ki67 was quantified by IHC from A549 tumor samples taken after 6 days of dosing; AZD0364 and selumetinib dosed simultaneously. **E,** Expression of selected RAS/MAPK-related transcripts over time, as quantified by qRT-PCR from A549 tumor samples taken after 6 days of dosing; AZD0364 and selumetinib dosed simultaneously. An experiment in A549 was run comparing different AZD0364 and selumetinib dosing schedules. **F,** Combined treatment of AZD0364 (once daily) and selumetinib (twice daily) is more efficacious than selumetinib (administered three times daily) treatment *in vivo* in A549 (mouse/group, $n = 12$) tumors. Combination dosing group reached 21% regression from baseline at day 21 and 38% regression from baseline at day 35. **G,** Intermittent dosing of the AZD0364 and selumetinib combination (dosed for 3.5 days every 4 days) resulted in tumor stasis (93% TGI at day 21), but not regression (mouse/group, $n = 12$). Tumors in continuous dosing group reach 21% regression from baseline at day 21. BiD, twice daily; QD, once daily. *P* value vs. vehicle: *, <0.05; **, <0.01; ***, <0.001; ****, <0.0001.

schedule was able to control tumor growth and lead to tumor stasis (TGI of 93% at 21 days postdosing). However, tumor regression was only achieved in the continuous dosing group (**Fig. 6G**). These data suggest continual RAS/MAPK pathway suppression is required for maximal efficacy.

Discussion

The RAS/MAPK signaling pathway is among the most frequently altered pathways in cancer. However, therapeutic activity of agents targeting individual nodes in this pathway has been linked to reactivation of the pathway via feedback loops and acquired resistance

mechanisms. Herein, we describe a potent and highly selective small-molecule ATP competitive inhibitor of ERK1/2, AZD0364. *In vitro*, treatment with AZD0364 resulted in dose- and time-dependent reduction of phosphorylation of ERK1/2 targets and potent inhibition of growth in multiple cancer cell lines, particularly those harboring mutations in the RAS/MAPK signaling pathway. In xenograft models, AZD0364 modulates downstream targets of ERK1/2 in a time- and dose-dependent manner, with full recovery to baseline levels upon cessation of dosing. We showed that the *in vitro* potency of AZD0364 translates to *in vivo* activity in three cell lines, A375, Calu-6, and A549, with maximum regression effect observed in the A375 melanoma cell line (potency order of AZD0364: A375, 0.059; Calu-6, 0.173; and A549, 0.32 μmol/L).

The clinical activity of single-agent RAS/MAPK pathway inhibitors has thus far been largely restricted to $BRAF^{V600E/K}$-mutant cancers. Reactivation of the pathway through mutation or changes in expression of MAPK proteins is a driver of resistance to BRAF inhibitors in $BRAF^{V600E/K}$-mutant melanoma (11, 34), and combined inhibition of RAF and MEK gives enhanced clinical benefit in this setting (14, 16, 17). Resistance continues to emerge through RAS/MAPK in this setting predominantly through *BRAF* amplification and mutations in *NRAS, KRAS, NF1*, and *MEK* (11, 12, 35, 36). Preclinical models of melanoma resistant to combined RAF/MEK inhibition are sensitive to ERK inhibition, and clinical activity of ERK inhibitors has been demonstrated in a subset of patients relapsing on BRAF and MEK therapy (25, 37). Thus, demonstrating that resistance mechanisms to this therapy maintain dependence on ERK signaling. Consistent with these data, in an A375 $BRAF^{V600E}$-mutant melanoma cell line with acquired resistance to inhibitors of BRAF and MEK1/2 grown as a xenograft, we have shown that AZD0364 treatment results in significant TGI. In this BRAF and MEK inhibitor acquired resistance setting, it remains an open question of whether an ERK inhibitor should be combined with a BRAF inhibitor or with other targeted therapies, such as a combination with BH3 mimetics, which we have recently shown to be active in preclinical models of melanoma (32).

In contrast to *BRAF*-mutant melanoma, there have been no clinical approvals for single-agent RAS/MAPK inhibitors in *RAS* mutation–driven cancers. Lack of efficacy can be driven by compensatory activation of other effector pathways, such as PI3K/AKT, but the major driver is thought to be incomplete RAS/MAPK pathway inhibition and subsequent reactivation of the pathway due to relief of negative feedback (18, 31, 38). Targeting the key effector kinase of the RAS/MAPK pathway through pharmacologic inhibition of ERK1/2 is a potential approach to mitigate the effects of this feedback reactivation (8, 20, 26), particularly when combined with other agents targeting the RAS/MAPK pathway, such as MEK inhibitors (28). As expected, AZD0364 reduced the growth of *KRAS*-mutant cancer cell lines, with a wide spectrum of response. In some cell lines, the sensitivity and duration of response were limited and coincident with pathway reactivation.

When AZD0364 and selumetinib were combined across a panel of KRAS-mutant NSCLC lines *in vitro*, a Loewe score of ≥5 (indicative of a synergistic combination response which is calculated to be greater than an additive combination effect) was identified in a number of cell lines, namely NCI-H2122, NCI-H358, A549, NCI-H1792, and NCI-H2009. However, a Loewe score of <5 does not necessarily indicate that combination treatment will not be beneficial in these lines. Where an inhibitor as a single agent already has a strong inhibitory effect on the RAS/MAPK pathway, a high Loewe synergy score is unlikely to be seen with combination treatment. For example, previously identified AZD0364-sensitive cell line, Calu-6, has a calculated Loewe synergy score of <5. Furthermore, the Loewe score is a measure of synergistic combination; a purely additive combination effect may still be sufficient to impact growth. In addition, the time frame of the assay (3 days) will not capture long-term effects of combination, in particular the potential for blocking or delaying the development of resistance which is seen with single-agent RAS/MAPK pathway inhibitors. Therefore, we speculate that combined AZD0364 and selumetinib treatment would also be beneficial in the models that are sensitive to monotherapy, as emerging resistance through pathway reactivation is likely to take place. The combination benefit of an ERK inhibitor with an MEK inhibitor translates to the *in vivo* preclinical experiments, where regressions are observed in the combination-treated groups in *KRAS*-mutant NSCLC cell lines identified from the *in vitro* screen when grown as xenografts; A549 and NCI-H358. Tumor regressions were also observed in the combination-treated groups in the *KRAS*-mutant colorectal cancer HCT-116 xenograft model.

Across a range of preclinical models, we have shown that there is a rationale to combine AZD0364 with selumetinib in patients with *KRAS*-mutant NSCLC. We acknowledge that a limiting factor of this clinical combination may be therapeutic margin, related to the on-target toxicity that is expected with an inhibitor of the RAS/MAPK pathway. Indeed, this was observed in a clinical trial combining the ERK inhibitor, GDC-0994, with the MEK inhibitor, cobimetinib (NCT02457793; ref. 39). These data highlight the need to explore alternative dosing regimens of combinations of MEK and ERK inhibitors that may alleviate the overlapping adverse effects. The predicted human half-life of AZD0364 is 7 hours, which will give flexibility in dosing regimen, allowing pathway recovery to improve combination tolerability. Preclinically, we show that intermittent dosing of the AZD0364 and selumetinib combination was better tolerated than the continuous schedule and resulted in TGI, which was marginally reduced compared with the continuous schedule. Thus, suggesting that intermittent dosing schedules may be a strategy to alleviate overlapping toxicities with these agents.

In summary, we have shown that AZD0364 is a potent and selective inhibitor of ERK1/2 signaling in preclinical models and can be combined with MEK1/2 inhibition to enhance activity in multiple preclinical models with RAS/MAPK pathway aberrations, concomitant with deeper suppression of pathway biomarkers.

Authors' Disclosures

E.J. Davies reports former employment with AstraZeneca and reports personal fees (shareholder) from AstraZeneca. L.C. Sandin reports a patent for royalty agreement with royalties paid from Alligator Bioscience AB. S.E. Willis reports personal fees from AstraZeneca (employment and shareholder) during the conduct of the study and outside the submitted work. M.P. Roudier reports employment with AstraZeneca at the time of the study. C. Rooney reports other from AstraZeneca (employment) outside the submitted work. M.J. Garnett reports grants from Wellcome Trust and AstraZeneca during the conduct of the study. S.E. Fawell reports employment with and personal fees (shareholder) from AstraZeneca. J.E. Pease reports other (salary and shares) from AstraZeneca outside the submitted work and has a patent for chemical entity patent issued (owner AstraZeneca). P.D. Smith reports employment with and personal fees (shareholder) from AstraZeneca outside the submitted work. No disclosures were reported by the other authors.

Authors' Contributions

V. Flemington: Conceptualization, formal analysis, investigation, methodology, writing–original draft, writing–review and editing. **E.J. Davies:** Conceptualization, formal analysis, validation, investigation, methodology, writing–original draft, writing–review and editing. **D. Robinson:** Investigation, visualization, methodology. **L.C. Sandin:** Investigation, visualization, methodology. **O. Delpuech:** Investigation, visualization, methodology. **P. Zhang:** Software, visualization,

methodology. **L. Hanson:** Investigation, visualization, methodology. **P. Farrington:** Investigation, visualization, methodology. **S. Bell:** Investigation, visualization, methodology. **K. Falenta:** Investigation, visualization, methodology. **F.D. Gibbons:** Formal analysis, investigation, visualization. **N. Lindsay:** Formal analysis, investigation, visualization. **A. Smith:** Investigation, methodology. **J. Wilson:** Investigation, methodology. **K. Roberts:** Investigation, methodology, writing–original draft. **M. Tonge:** Investigation, visualization. **P. Hopcroft:** Investigation, visualization. **S.E. Willis:** Validation, investigation. **M.P. Roudier:** Formal analysis, validation, investigation, visualization, methodology. **C. Rooney:** Validation, methodology. **E.A. Coker:** Validation, investigation. **P. Jaaks:** Validation, investigation. **M.J. Garnett:** Supervision, methodology. **S.E. Fawell:** Supervision. **C.D. Jones:** Supervision. **R.A. Ward:** Conceptualization, validation, methodology. **I. Simpson:** Conceptualization, validation. **S.C. Cosulich:** Supervision, writing–review and editing. **J.E. Pease:** Conceptualization, supervision. **P.D. Smith:** Conceptualization, supervision, writing–review and editing.

Acknowledgments

We thank all staff at animal science technology in Alderley Park for technical support with *in vivo* experiments and the Genomics of Drug Sensitivity in Cancer screening team for genomic characterization of the cell lines in the 72-hour cell proliferation screen of 747 cancer cell lines. We would also like to thank Ben Sidders for reanalysis of data and formatting of figures and Nicolas Floc'h for critical review of the article.

The costs of publication of this article were defrayed in part by the payment of page charges. This article must therefore be hereby marked *advertisement* in accordance with 18 U.S.C. Section 1734 solely to indicate this fact.

Received January 7, 2020; revised July 13, 2020; accepted November 6, 2020; published first December 3, 2020.

References

1. Balmanno K, Cook SJ. Tumour cell survival signalling by the ERK1/2 pathway. Cell Death Differ 2009;16:368–77.
2. Meloche S, Pouyssegur J. The ERK1/2 mitogen-activated protein kinase pathway as a master regulator of the G1- to S-phase transition. Oncogene 2007;26:3227–39.
3. Unal EB, Uhlitz F, Bluthgen N. A compendium of ERK targets. FEBS Lett 2017; 591:2607–15.
4. Bos JL. ras oncogenes in human cancer: a review. Cancer Res 1989;49:4682–9.
5. Hobbs GA, Der CJ, Rossman KL. RAS isoforms and mutations in cancer at a glance. J Cell Sci 2016;129:1287–92.
6. Holderfield M, Deuker MM, McCormick F, McMahon M. Targeting RAF kinases for cancer therapy: BRAF-mutated melanoma and beyond. Nat Rev Cancer 2014;14:455–67.
7. Caunt CJ, Sale MJ, Smith PD, Cook SJ. MEK1 and MEK2 inhibitors and cancer therapy: the long and winding road. Nat Rev Cancer 2015;15:577–92.
8. Roskoski R Jr. Targeting ERK1/2 protein-serine/threonine kinases in human cancers. Pharmacol Res 2019;142:151–68.
9. Wright CJ, McCormack PL. Trametinib: first global approval. Drugs 2013;73: 1245–54.
10. Nazarian R, Shi H, Wang Qi, Kong X, Koya RC, Lee H, et al. Melanomas acquire resistance to B-RAF(V600E) inhibition by RTK or N-RAS upregulation. Nature 2010;468:973–7.
11. Johnson DB, Menzies AM, Zimmer L, Eroglu Z, Ye F, Zhao S, et al. Acquired BRAF inhibitor resistance: a multicenter meta-analysis of the spectrum and frequencies, clinical behaviour, and phenotypic associations of resistance mechanisms. Eur J Cancer 2015;51:2792–9.
12. Nissan MH, Pratilas CA, Jones AM, Ramirez R, Won H, Liu C, et al. Loss of NF1 in cutaneous melanoma is associated with RAS activation and MEK dependence. Cancer Res 2014;74:2340–50.
13. Dummer R, Ascierto PA, Gogas HJ, Arance A, Mandala M, Liszkay G, et al. Encorafenib plus binimetinib versus vemurafenib or encorafenib in patients with BRAF-mutant melanoma (COLUMBUS): a multicentre, open-label, randomised phase 3 trial. Lancet Oncol 2018;19:603–15.
14. Flaherty KT, Infante JR, Daud A, Gonzalez R, Kefford RF, Sosman J, et al. Combined BRAF and MEK inhibition in melanoma with BRAF V600 mutations. N Engl J Med 2012;367:1694–703.
15. Odogwu L, Mathieu L, Blumenthal G, Larkins E, Goldberg KB, Griffin N, et al. FDA approval summary: dabrafenib and trametinib for the treatment of metastatic non-small cell lung cancers harboring BRAF V600E mutations. Oncologist 2018;23:740–5.
16. Larkin J, Ascierto PA, Dréno B, Atkinson V, Liszkay G, Maio M, et al. Combined vemurafenib and cobimetinib in BRAF-mutated melanoma. N Engl J Med 2014; 371:1867–76.
17. Long GV, Stroyakovskiy D, Gogas H, Levchenko E, de Braud F, Larkin J, et al. Combined BRAF and MEK inhibition versus BRAF inhibition alone in melanoma. N Engl J Med 2014;371:1877–88.
18. Lito P, Saborowski A, Yue J, Solomon M, Joseph E, Gadal S, et al. Disruption of CRAF-mediated MEK activation is required for effective MEK inhibition in KRAS mutant tumors. Cancer Cell 2014;25:697–710.
19. Little AS, Balmanno K, Sale MJ, Smith PD, Cook SJ. Tumour cell responses to MEK1/2 inhibitors: acquired resistance and pathway remodelling. Biochem Soc Trans 2012;40:73–8.
20. Smalley I, Smalley KSM. ERK inhibition: a new front in the war against MAPK pathway-driven cancers? Cancer Discov 2018;8:140–2.
21. Ahronian LG, Sennott EM, Van Allen EM, Wagle N, Kwak EL, Faris JE, et al. Clinical acquired resistance to RAF inhibitor combinations in BRAF-mutant colorectal cancer through MAPK pathway alterations. Cancer Discov 2015;5: 358–67.
22. Ward RA, Colclough N, Challinor M, Debreczeni JE, Eckersley K, Fairley G, et al. Structure-guided design of highly selective and potent covalent inhibitors of ERK1/2. J Med Chem 2015;58:4790–801.
23. Ward RA, Anderton MJ, Bethel P, Breed J, Cook C, Davies EJ, et al. Discovery of a potent and selective oral inhibitor of ERK1/2 (AZD0364) that is efficacious in both monotherapy and combination therapy in models of NSCLC. J Med Chem 2019;62:11004–18.
24. Ward RA, Bethel P, Cook C, Davies E, Debreczeni JE, Fairley G, et al. Structure-guided discovery of potent and selective inhibitors of ERK1/2 from a modestly active and promiscuous chemical start point. J Med Chem 2017; 60:3438–50.
25. Moschos SJ, Sullivan RJ, Hwu W-J, Ramanathan RK, Adjei AA, Fong PC, et al. Development of MK-8353, an orally administered ERK1/2 inhibitor, in patients with advanced solid tumors. JCI Insight 2018;3:e92352.
26. Germann UA, Furey BF, Markland W, Hoover RR, Aronov AM, Roix JJ, et al. Targeting the MAPK signaling pathway in cancer: promising preclinical activity with the novel selective ERK1/2 inhibitor BVD-523 (ulixertinib). Mol Cancer Ther 2017;16:2351–63.
27. Vial E, Marshall CJ. Elevated ERK-MAP kinase activity protects the FOS family member FRA-1 against proteasomal degradation in colon carcinoma cells. J Cell Sci 2003;116:4957–63.
28. Merchant M, Moffat J, Schaefer G, Chan J, Wang Xi, Orr C, et al. Combined MEK and ERK inhibition overcomes therapy-mediated pathway reactivation in RAS mutant tumors. PLoS One 2017;12:e0185862.
29. Yang W, Soares J, Greninger P, Edelman EJ, Lightfoot H, Forbes S, et al. Genomics of Drug Sensitivity in Cancer (GDSC): a resource for therapeutic biomarker discovery in cancer cells. Nucleic Acids Res 2013;41: D955–61.
30. Dry JR, Pavey S, Pratilas CA, Harbron C, Runswick S, Hodgson D, et al. Transcriptional pathway signatures predict MEK addiction and response to selumetinib (AZD6244). Cancer Res 2010;70:2264–73.
31. Pratilas CA, Taylor BS, Ye Q, Viale A, Sander C, Solit DB, et al. (V600E) BRAF is associated with disabled feedback inhibition of RAF-MEK signaling and elevated transcriptional output of the pathway. Proc Natl Acad Sci U S A 2009;106:4519–24.
32. Sale MJ, Minihane E, Monks NR, Gilley R, Richards FM, Schifferli KP, et al. Targeting melanoma's MCL1 bias unleashes the apoptotic potential of BRAF and ERK1/2 pathway inhibitors. Nat Commun 2019;10:5167.
33. Skoulidis F, Byers LA, Diao L, Papadimitrakopoulou VA, Tong P, Izzo J, et al. Co-occurring genomic alterations define major subsets of KRAS-mutant lung adenocarcinoma with distinct biology, immune profiles, and therapeutic vulnerabilities. Cancer Discov 2015;5:860–77.
34. Shi H, Hugo W, Kong X, Hong A, Koya RC, Moriceau G, et al. Acquired resistance and clonal evolution in melanoma during BRAF inhibitor therapy. Cancer Discov 2014;4:80–93.

35. Long GV, Fung C, Menzies AM, Pupo GM, Carlino MS, Hyman J, et al. Increased MAPK reactivation in early resistance to dabrafenib/trametinib combination therapy of BRAF-mutant metastatic melanoma. Nat Commun 2014;5:5694.
36. Wagle N, Van Allen EM, Treacy DJ, Frederick DT, Cooper ZA, Taylor-Weiner A, et al. MAP kinase pathway alterations in BRAF-mutant melanoma patients with acquired resistance to combined RAF/MEK inhibition. Cancer Discov 2014;4:61–8.
37. Sullivan RJ, Infante JR, Janku F, Wong DJL, Sosman JA, Keedy V, et al. First-in-class ERK1/2 inhibitor Ulixertinib (BVD-523) in patients with MAPK mutant advanced solid tumors: results of a phase I dose-escalation and expansion study. Cancer Discov 2018;8:184–95.
38. Friday BB, Yu C, Dy GK, Smith PD, Wang L, Thibodeau SN, et al. BRAF V600E disrupts AZD6244-induced abrogation of negative feedback pathways between extracellular signal-regulated kinase and Raf proteins. Cancer Res 2008;68:6145–53.
39. Weekes C, Lockhart A, LoRusso P, Murray E, Park E, Tagen M, et al. A phase Ib study to evaluate the MEK inhibitor cobimetinib in combination with the ERK1/2 inhibitor GDC-0994 in patients with advanced solid tumors [abstract]. In: Proceedings of the American Association for Cancer Research Annual Meeting 2017; 2017 Apr 1–5; Washington, DC. Philadelphia (PA): AACR; 2017. Abstract nr CT107.